ChemComm

COMMUNICATION

View Article Online
View Journal

Check for updates

Cite this: DOI: 10.1039/c9cc09595k

Received 10th December 2019,
Accepted 10th March 2020

DOI: 10.1039/c9cc09595k

rsc.li/chemcomm

Published on 10 March 2020. Downloaded by Uppsala University on 3/17/2020 5:39:14 PM.

A phenotypic approach to probing cellular outcomes using heterobivalent constructs†

Rohit Bhadoria, Kefeng Ping, Christer Lohk,‡ Ivar Järving and Pavel Starkov *

Various conjugation techniques are used to affect the intracellular delivery of bioactive small molecules. However, the ability to track changes in the phenotype when applying these tools remains poorly studied. We addressed this issue by having prepared a focused library of heterobivalent constructs based on Rho kinase inhibitor HA-100. By comparing the induction of the phenotype of interest, cell viability and cellular uptake, we demonstrate that various conjugates indeed lead to divergent cellular outcomes.

Cell permeability is one of the biggest challenges faced when developing multifunctional and high-molecular-weight chemical probes.[1–8] This can be improved by installing moieties that help the constructs internalize, including cell-penetrating peptides[4,5] and chemical modifications by fatty acids, cholesterol, asparagusic and lipoic acids.[7,8] While some of the cellular uptake-enhancing end-groups have been shown to target treatment-resistant cancer cells and bacteria more effectively,[9,10] it remains poorly understood whether and how such end-groups may alter the cell-biological outcome at the phenotypic level.

Cellular uptake is often assessed by using constructs that incorporate a fluorescent probe, which also serves as a cargo.[11–14] This strategy has proven to be highly valuable for identification and studying the mechanisms of cellular uptake.[9–14] However, it does not unambiguously demonstrate whether increased cell permeability directly translates into sustained intracellular activity. Instead of employing fluorescently labelled compounds as cargoes, it may, perhaps, be more insightful to visualise cellular outcomes by cell staining techniques. This approach relies on comparing holistic changes in acquired *vs.* the default phenotype, for instance, changes in cell and organelle morphology, cytoskeletal rearrangements or defects in cell division (Fig. 1).[15]

We address the question of whether several known chemical modifiers of cellular uptake (the end-groups) are only responsible for getting small-molecule-cargo inside the cell or whether they may also influence the overall cell-biological outcome.

Herein, we establish a chemically straightforward platform to evaluate a focused library of heterobivalent compounds by equipping small molecules, which induce well-characterised phenotypes, with different end-groups. In this work, we employ a polyethyleneglycol (PEG) linker 4,7,10-trioxa-1,13-tridecanediamine to ensure that the biomolecular interactions between the

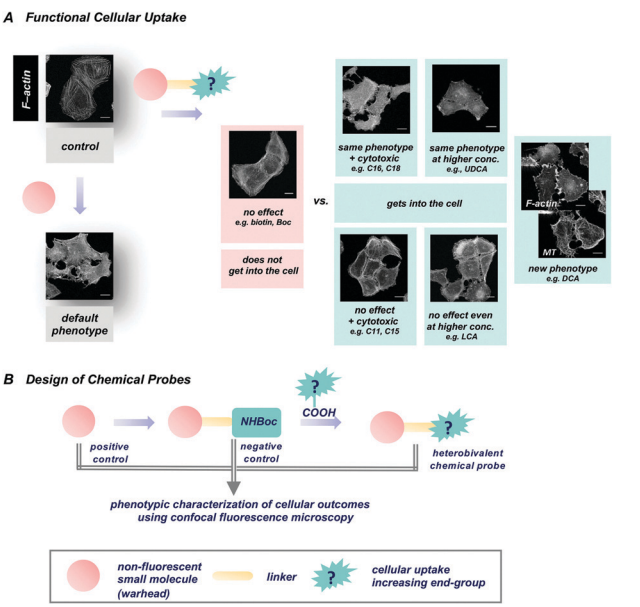

Fig. 1 (A) Functional cellular uptake based on non-fluorescent heterobivalent conjugates and changes in induced phenotypes visualized by cell staining. (B) Design of bifunctional probes that are supplemented by positive and negative controls. Scale bars, 20 μm.

Department of Chemistry & Biotechnology, Tallinn University of Technology, 12618 Tallinn, Estonia. E-mail: pavel.starkov@taltech.ee

† Electronic supplementary information (ESI) available: Cell culture methods and materials, cell imaging and quantification, cell viability and kinase assays, synthetic procedures and characterisation of compounds. See DOI: 10.1039/c9cc09595k

‡ Current address: Master's Program in Biomedical Engineering, University of Paris, 75006 Paris, France.

Published on 10 March 2020. Downloaded by Uppsala University on 3/17/2020 5:39:14 PM.

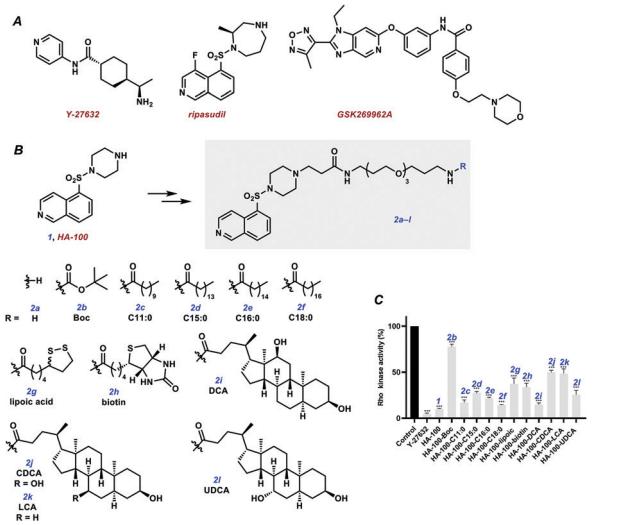

Fig. 2 Heterobivalent Rho kinase inhibition probes. (A) Small molecule Rho kinase inhibitors Y-27632, ripasudil and GSK269962A. (B) Heterobivalent constructs derived from HA-100 used in this study. (C) ROCK2 kinase activity inhibition by Y-27632 (50 μM) and HA-100 (100 μM) and HA-100 heterobivalent probes **2c–2l** (100 μM). One-way ANOVA followed by Bonferroni post-hoc test: ***$p < 0.001$ *vs.* control, (mean + S.D.; $n = 3$).

'warhead' and the target remain undisturbed even in the close proximity of other biologically functional moieties.[16–18]

First, we turned our attention to Rho-associated coiled-coil-containing protein kinase (ROCK) inhibitors. In mammalian cells, there are two ROCK isoforms (ROCK1 and ROCK2), which are instrumental in a myriad of cellular processes and dysregulation of which is implicated in a wide spectrum of diseases.[19] To date, several classes of ROCK inhibitors have been developed.[20] Their scaffolds are chemically diverse (Fig. 2A), and we have focused our efforts on modifying HA-100 (**1**) because of the ease of chemical modification (*i.e.* linker extension and end-group attachment) (Fig. 2B).[21]

The chemical extension of HA-100 was carried out by Michael addition of **1** to ethyl acrylate, hydrolysis of the resulting ester and subsequent direct carboxamidation with a monoprotected 4,7,10-trioxa-1,13-tridecanediamine to give linker-extended Boc-protected precursor **2b**. It was then *N*-deprotected to give free amine **2a**, which was coupled with corresponding unprotected carboxylic acids (*i.e.* fatty and bile acids, lipoic acid and biotin) to give a library of compounds (**2c–2l**).[22] All compounds were subjected to the Rho kinase assay to confirm they inhibited ROCK2 kinase activity (Fig. 2C).

The final constructs (**2c–2l**) were then assessed at different concentrations and time durations in human osteosarcoma (U2OS) cell line (Fig. 3A). The inhibition of Rho kinase is known to lead to a pronounced reduction in stress fibres – the bundles of filamentous actin (F-actin) – along with the characteristic changes in cell shape.[23] If linker-extended constructs **2c–2l** were both cell permeable and functional, we would expect to observe this default phenotype. Several well-established Rho kinase inhibitors (Y-27632, GSK269962A, and HA-100) were used as positive controls.

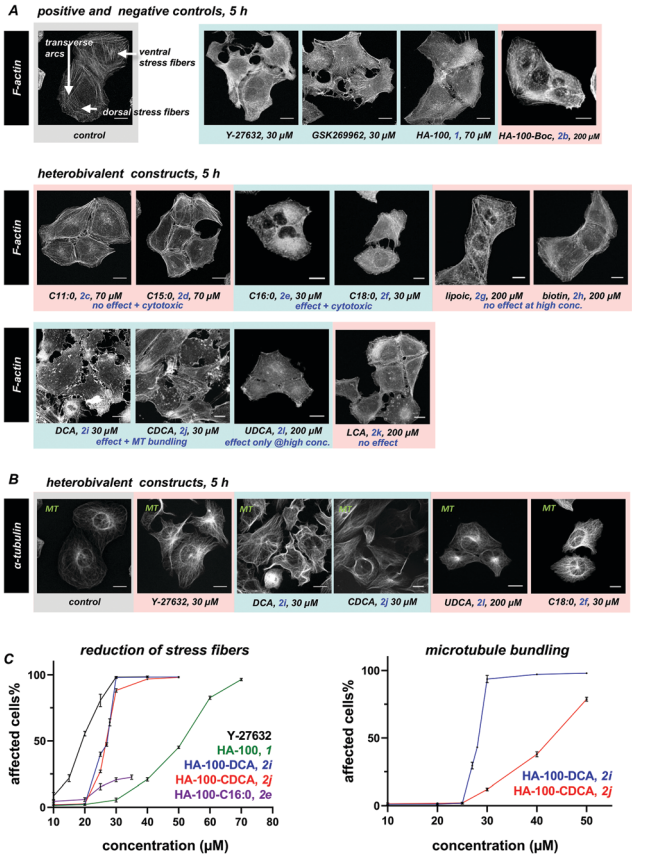

Fig. 3 Different heterobivalent constructs lead to divergent phenotypes. U2OS cells were treated with compounds for 5 h and stained for F-actin (A) and α-tubulin (B). Green fluorescence (FITC, λ_{ex} = 488 nm, λ_{em} = 498–551 nm), red fluorescence (TRITC, λ_{ex} = 561 nm, λ_{em} = 569–622 nm). (C) Quantification of the number of cells with altered organization of F-actin (left) and microtubules (right) for selected HA-100 constructs. (mean + S.D.; $n = 3$). For cell viability data, see Fig. S1 and Tables S1 and S2, ESI.† Scale bars, 20 μm.

Compounds **2c** and **2d**, with C11:0 and C15:0 end-groups, respectively, did not induce the desired phenotype even at prolonged treatment times and were toxic at higher concentrations (Tables S1 and S2, ESI†). Palmitic (C16:0; **2e**) and stearic acid (C18:0; **2f**) constructs did induce the phenotype of interest, albeit after rounds of optimisations (time *vs.* concentration). The initial treatment over 14 h with 20 μM of **2e** and **2f** did not lead to dissolution of stress fibres, whereas at 30 μM both of the constructs resulted in cell death (no cells observed). Once the duration of treatment was reduced to 5 h, we were able to observe the phenotype of interest for both compounds (**2e** and **2f** at 30 μM). However, high cytotoxicity of these constructs has encouraged us to look for the alternatives (for cell viability data, see Fig. S1 and Tables S1 and S2, ESI†).

Under standard U2OS cell culture conditions (DMEM, 10% FBS; 1% P/S), lipoic acid[11]-conjugate **2g** was found ineffective (5 h; 200 μM). The biotin construct (**2h**), a conjugation tool often used in biochemical follow-up studies,[24] also proved inactive (5 h; 200 μM).

We have also profiled a selection of bile acid conjugates (**2i–2l**). Bile acids belong to a class of cholesterol derivatives

This journal is © The Royal Society of Chemistry 2020

Published on 10 March 2020. Downloaded by Uppsala University on 3/17/2020 5:39:14 PM.

known to facilitate digestion and absorption of lipids in vertebrates.[25,26] Although conjugation to bile acids is often overlooked, they may hold the potential to improve cellular uptake. First, bile acid conjugation is primarily used to target and increase uptake of the constructs in the liver, biliary tract and the intestines cell lines.[27] Second, bile acids are chemically diverse and can be modified to incorporate additional labelling tags. Third, albeit they are structurally quite similar, they are known to lead to divergent cell biological effects.[28]

Out of the four profiled bile acids, derivatives of deoxycholic (DCA; **2i**), chenodeoxycholic (CDCA; **2j**) and ursodeoxycholic acids (UDCA; **2l**, albeit at higher concentration) brought about the desired phenotypic changes, whereas the lithocholic acid conjugate did not (LCA; **2k**; 5 h; tested up to 200 μM). We also confirmed that the blank bile acid–PEG constructs did not lead to reduction in stress fibres on their own (Fig. S3, ESI†).

To quantify the effects observed, we counted the number of cells that have acquired the desired phenotype at different concentrations of HA-100 and its conjugates with C16:0 (**2e**), DCA (**2i**), and CDCA (**2j**), and Y-27632, the most used Rho inhibitor (Fig. 3C). Compounds with the DCA and CDCA end-groups had higher activity than HA-100. The effect of palmitic acid construct **2e** could not be quantified beyond 35 μM as it was cytotoxic and no cells were observed on coverslips (*cf.* Tables S1 and S2, ESI†).

Importantly, we have observed a secondary effect on the organisation of microtubules (Fig. 3C). DCA and CDCA conjugates **2i** and **2j** both induced bundling of microtubules, whereas compound **2i** induced abrupt change in the number of affected cells when its concentration was increased from 25 μM to 30 μM. Although we cannot rule out synergistic effects of our bifunctional constructs, it is known that actin cytoskeletal rearrangements have a crosstalk effect on microtubules.[29]

Next, we wished to test whether these modifications would also work with another kinase inhibitor (Fig. 4). We looked into direct inhibition of myosin light chain kinase (MLCK/MYLK), which phosphorylates myosin light chain (MLC).[30] We modified inhibitor ML-7 (**4**),[31] which is structurally akin to HA-100 (**1**). Treating the cells with **4** is known to have a pronounced effect on F-actin/p-MLC colocalization and cell shape.[32,33] Indeed, the parent compound (**4**) and its conjugates ML-7-C16:0 (**5b**) ML-7-DCA (**5c**) and ML-7-CDCA (**5d**) have led to similar changes in F-actin (*i.e.* dissolution of stress fibres) and in intracellular distribution of phospho-MLC2 (Ser19) (p-MLC).[34] We quantified the effects of ML-7 and its derivatives on the organisation of F-actin and microtubules (Fig. 4C). While the C16:0 construct (**5b**) performed similarly to the parent compound, the DCA (**5c**) and CDCA (**5d**) conjugates led to reduction of stress fibres at lower concentration. However, both **5c** and **5d** also induced microtubule bundling (Fig. S4, ESI†). Notably, ML-7 and its derivatives do not lead to the reduction of p-MLC in the cell periphery, which indicates that the effect on actomyosin is achieved through inhibition of MLCK and not ROCK (*cf.* Rho kinase inhibitor GSK269962A *vs.* ML-7; arrows in Fig. 4B and Fig. S2, ESI†).[35] Interestingly, unlike the case of Rho kinase inhibitor HA-100, the C16:0 construct of ML-7 is less

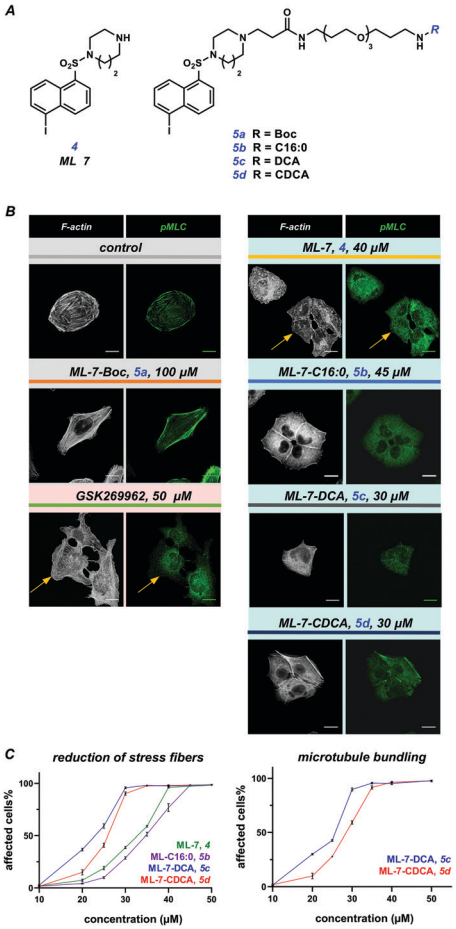

Fig. 4 Effects of myosin light chain kinase inhibitor ML-7-based constructs. (A) Chemical identity of ML-7 constructs. (B) Comparison of cells treated by either ROCK or MYLK inhibitors. U2OS cells were treated with compounds for 5 h and stained for F-actin (colourless) and p-MLC (green). Green fluorescence (Alexa 488, λ_{ex} = 488 nm, λ_{em} = 498–551 nm), red fluorescence (TRITC, λ_{ex} = 561 nm, λ_{em} = 569–622 nm). (C) Quantification of the number of cells with altered organization of F-actin (left) and microtubules (right) by ML-7 constructs (mean + S.D.; n = 3). Scale bars, 20 μm.

toxic than the parent compound or other conjugates (Tables S1 and S2, ESI†).

With several constructs demonstrating that conjugation to bile and fatty acids results in different outcomes, we wished to see to what extent the end-groups affect cell permeability. We prepared fluorescent probes based on 7-dimethylaminocoumarin-4-acetic acid (DMACA; Fig. 5). Both benzylamide of DMACA **6a** and linker-extended *N*-Boc protected construct **6b** did not internalise, while C16:0, DCA and CDCA conjugates (**6c** > **6d** > **6e**) did. For compounds **6d** and **6e**, the efficiency of cellular uptake correlated with the onset of changes in phenotypes (Fig. 3C and 4C).

Having screened the two focused libraries of heterobifunctional probes using well-established ROCK and MYLK inhibitors, we observe that there are complex relationships between the drug cores (warheads), the end-groups and the final heterobifunctional constructs themselves. In addition to inducing the desired phenotype, we show that such combinations may also lead to the

Published on 10 March 2020. Downloaded by Uppsala University on 3/17/2020 5:39:14 PM.

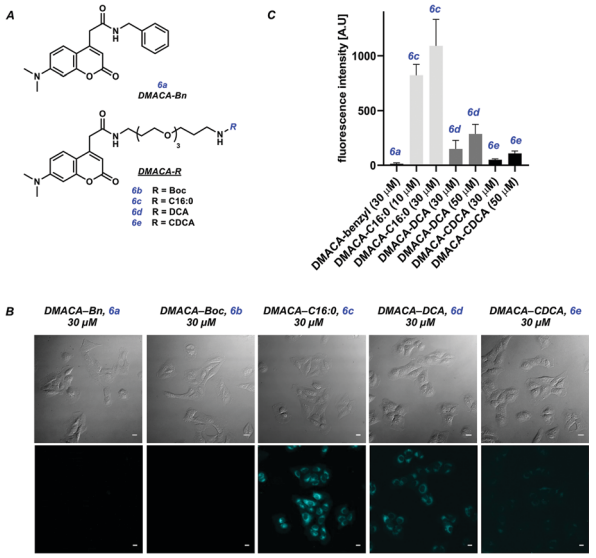

Fig. 5 Qualitative and quantitative comparison of cellular uptake of heterobivalent constructs. (A) Chemical identity of DMACA constructs tested. (B) Confocal images for DMACA constructs at 30 μM (DIC and λ_{ex} = 405 nm, λ_{em} = 435–478 nm). (C) Mean cellular fluorescence of cells treated with DMACA constructs (mean + S.D.; n = 3). U2OS cells were treated with compounds, after 1 h medium was exchanged and the cells were imaged live on confocal microscope. Scale bars, 20 μm.

secondary effects (induction of microtubule bundling) and the variations in cytotoxicity and cellular uptake. In order to quantitatively predict the structure–activity relationships and to better understand the underlying molecular mechanisms, a larger subset of modified small molecules, including allosteric inhibitors, and modifiers (the end-groups) would be needed.

In conclusion, we have developed a confocal microscopy-based assay for the 'in-cell' screening of heterobivalent constructs. This approach can be used to distinguish between various constructs, even if their chemical alterations are very minute. We have shown that both the end-groups and the warheads contribute to the overall cellular outcome.

This research was funded by Estonian Research Council Grant PUT1290 and TalTech Young Investigator Grant B62 (both to P. S.). Tallinn HRMS facilities are supported by Institutional Research Funding IUT19-9 of the Estonian Ministry for Education & Research. We thank COST Action CA15135 MuTaLig members, Dr Pirjo Spuul (Tallinn) for helpful discussions, and Mika Molin and Marko Crivaro for technical assistance at the University of Helsinki Light Microscopy Unit. K. P. acknowledges Estonian Smart Specialization PhD Fellowship.

Conflicts of interest

There are no conflicts to declare.

Notes and references

1 C. H. Arrowsmith, J. E. Audia, C. Austin, J. Baell, J. Bennett, J. Blagg, C. Bountra, P. E. Brennan, P. J. Brown, M. E. Bunnage, C. Buser-Doepner, R. M. Campbell, A. J. Carter, P. Cohen, R. A. Copeland, B. Cravatt, J. L. Dahlin, D. Dhanak, A. M. Edwards, M. Frederiksen, S. V. Frye, N. Gray, C. E. Grimshaw, D. Hepworth, T. Howe, K. V. M. Huber, J. Jin, S. Knapp, J. D. Kotz, R. G. Kruger, D. Lowe, M. M. Mader, M. Marsden, A. Mueller-Fahrnow, S. Müller, R. C. O'Hagan, J. P. Overington, D. R. Owen, S. H. Rosenberg, R. Ross, B. Roth, M. Schapira, S. L. Schreiber, B. Shoichet, M. Sundström, G. Superti-Furga, J. Taunton, L. Toledo-Sherman, C. Walpole, M. A. Walters, T. M. Willson, P. Workman, R. N. Young and W. J. Zuercher, *Nat. Chem. Biol.*, 2015, **11**, 536.
2 N. J. Yang and M. J. Hinner, *Methods Mol. Biol.*, 2015, **1266**, 29.
3 S. D. Conner and S. L. Schmid, *Nature*, 2003, **422**, 37.
4 K. M. Stewart, K. L. Horton and S. O. Kelley, *Org. Biomol. Chem.*, 2008, **6**, 2242.
5 G. Guidotti, L. Brambilla and D. Rossi, *Trends Pharmacol. Sci.*, 2017, **38**, 406.
6 J. Mosquera, I. García and L. M. Liz-Marzán, *Acc. Chem. Res.*, 2018, **51**, 2305.
7 G. Gasparini, E.-K. Bang, J. Montenegro and S. Matile, *Chem. Commun.*, 2015, **51**, 10389.
8 M. Avadisian and P. T. Gunning, *Mol. BioSyst.*, 2013, **9**, 2179.
9 C. J. McKinlay, R. M. Waymouth and P. A. Wender, *J. Am. Chem. Soc.*, 2016, **138**, 3510.
10 A. Antonoplis, X. Zang, M. A. Huttner, K. K. L. Chong, Y. B. Lee, J. Y. Co, M. R. Amieva, K. A. Kline, P. A. Wender and L. Cegelski, *J. Am. Chem. Soc.*, 2018, **140**, 16140.
11 G. Gasparini, G. Sargsyan, E.-K. Bang, N. Sakai and S. Matile, *Angew. Chem., Int. Ed.*, 2015, **54**, 7328.
12 A. Nagel, P. S. Raschle and H. Wennemers, *Angew. Chem., Int. Ed.*, 2017, **56**, 122.
13 G. H. Bird, E. Mazzola, K. Opoku-Nsiah, M. A. Lammert, M. Godes, D. S. Neuberg and L. D. Walensky, *Nat. Chem. Biol.*, 2016, **12**, 845.
14 D. Zhang, L. Wei, M. Zhong, L. Xiao, H.-W. Li and J. Wang, *Chem. Sci.*, 2018, **9**, 5260.
15 U. S. Eggert, *Nat. Chem. Biol.*, 2013, **9**, 206.
16 B. Z. Stanton, E. J. Chory and G. R. Crabtree, *Science*, 2018, **359**, eaao5902.
17 T. W. Corson, N. Aberle and C. M. Crews, *ACS Chem. Biol.*, 2008, **3**, 677.
18 C. Borsari, D. J. Trader, A. Tait and M. P. Costi, *J. Med. Chem.*, 2020, **63**, DOI: 10.1021/acs.jmedchem.9b01456.
19 K. Riento and A. J. Ridley, *Nat. Rev. Mol. Cell Biol.*, 2003, **4**, 446.
20 Y. Feng, P. V. LoGrasso, O. Defert and R. Li, *J. Med. Chem.*, 2016, **59**, 2269.
21 S. P. Davies, H. Reddy, M. Caivano and P. Cohen, *Biochem. J.*, 2000, **351**, 95.
22 R. M. Lanigan, V. Karaluka, M. T. Sabatini, P. Starkov, M. Badland, L. Boulton and T. D. Sheppard, *Chem. Commun.*, 2016, **52**, 8846.
23 S. Pellegrin and H. Mellor, *J. Cell Sci.*, 2007, **120**, 3491.
24 B. Lomenick, R. W. Olsen and J. Huang, *ACS Chem. Biol.*, 2011, **6**, 34.
25 F. G. Schaap, M. Trauner and P. L. Jansen, *Nat. Rev. Gastroenterol. Hepatol.*, 2014, **11**, 55.
26 S. Zhuang, Q. Li, L. Cai, C. Wang and X. Lei, *ACS Cent. Sci.*, 2017, **3**, 501.
27 C. Faustino, C. Serafim, P. Rijo and C. Pinto Reis, *Expert Opin. Drug Delivery*, 2016, **13**, 1133.
28 J. D. Martinez, E. D. Stratagoules, J. M. LaRue, A. A. Powell, P. R. Gause, M. T. Craven, C. M. Payne, M. B. Powell, E. W. Gerner and D. L. Earnest, *Nutr. Cancer*, 1998, **31**, 111.
29 A. Takesono, S. J. Heasman, B. Wojciak-Stothard, R. Garg and A. J. Ridley, *PLoS One*, 2010, **5**, e8774.
30 F. Hong, B. D. Haldeman, D. Jackson, M. Carter, J. E. Baker and C. R. Cremo, *Arch. Biochem. Biophys.*, 2011, **510**, 135.
31 M. Saitoh, T. Ishikawa, S. Matsushima, M. Naka and H. Hidaka, *J. Biol. Chem.*, 1987, **262**, 7796.
32 Y. Li, D. Lovett, Q. Zhang, S. Neelam, R. A. Kuchibhotla, R. Zhu, G. G. Gundersen, T. P. Lele and R. B. Dickinson, *Biophys. J.*, 2015, **109**, 670.
33 S. B. Khatau, C. M. Hale, P. J. Stewart-Hutchinson, M. S. Patel, C. L. Stewart, P. C. Searson, D. Hodzic and D. Wirtz, *Proc. Natl. Acad. Sci. U. S. A.*, 2009, **106**, 19017.
34 K. Katoh, Y. Kano and Y. Noda, *J. R. Soc., Interface*, 2011, **8**, 305.
35 G. Totsukawa, Y. Yamakita, S. Yamashiro, D. J. Hartshorne, Y. Sasaki and F. Matsumura, *J. Cell Biol.*, 2000, **154**, 797.

 This journal is © The Royal Society of Chemistry 2020